Available online at www.sciencedirect.com
SCIENCE DIRECT®
PERGAMON
Solid State Communications 128 (2003) 35–39
solid state communications
www.elsevier.com/locate/ssc

Effect of isotopic mass on the photoluminescence spectra of zinc oxide

F.J. Manjón[a,*], M. Mollar[a], M.A. Hernández-Fenollosa[a], B. Marí[a], R. Lauck[b], M. Cardona[b]

[a]*Dpto. de Física Aplicada, Universitat Politècnica de València, Valencia, Spain*
[b]*Max-Planck-Institut für Festkörperforschung, Heisenbergstr. 1, D-70569 Stuttgart, Germany*

Received 1 July 2003; received in revised form 2 July 2003; accepted 4 July 2003 by J. Kuhl

Abstract

ZnO is a wurtzite-type semiconductor at ambient conditions whose natural composition consists of almost pure ^{16}O and a mixture of 48.6% ^{64}Zn, 27.9% ^{66}Zn, 4.1% ^{67}Zn, 18.8% ^{68}Zn, and 0.6% ^{70}Zn. In this work, we report a photoluminescence study of different samples of isotopically pure and natural zinc oxide between 15 and 300 K. The isotopic coefficients of the bound exciton energy have been obtained and compared with previous values for the shift of the free A exciton energy. The isotopic coefficients of the bound exciton energy have allowed us to estimate the contribution of the zinc and the oxygen vibrations to the bandgap renormalization by electron–phonon interaction. A two-oscillator model based on the zinc and oxygen renormalization energies has been used to account for the temperature dependence of the bandgap in ZnO.

PACS: 71.20.Nr

Keywords: A. Zinc oxide; A. II–VI Semiconductors; D. Low temperature; E. Photoluminescence

1. Introduction

Zinc oxide (ZnO) at ambient conditions is a wurtzite-type semiconductor with a fundamental band gap of around 3.4 eV at low temperature and is an important material in a broad range of applications [1]. Unintentionally doped ZnO is n-type and usually exhibits a large free electron concentration due to the presence of unbalanced donor and acceptor impurities. These impurities are responsible for the different colors shown by ZnO crystals, which usually range from colorless to pale yellow and even dark brown. The natural abundance of O is mainly of 99.8% ^{16}O and 0.2% ^{18}O; i.e. nearly pure ^{16}O. The natural abundance of Zn is 48.6% ^{64}Zn, 27.9% ^{66}Zn, 4.1% ^{67}Zn, 18.8% ^{68}Zn, and 0.6% ^{70}Zn. Therefore, in the spirit of the virtual crystal approximation, the average natural composition of ZnO ($^{nat}Zn^{16}O$) will be assumed to be $^{65.4}Zn^{16}O$.

It is well-known that the bandgap energy of semiconductors depends on the average isotopic mass [2,3]. This dependence has already been observed for ZnO in previous works [4–6]. In these works, only four different isotopic compositions were used and isotopic bandgap shifts were measured by photoluminescence (PL) and/or optical reflectivity methods. In the present work, we report a comprehensive study of the PL of seven unintentionally doped ZnO samples with different isotopic compositions, performed at temperatures between 15 and 300 K. Our main interest was the investigation of the shift of the PL features with the isotopic masses in order to obtain the isotopic contributions of zinc and oxygen to the electron–phonon renormalization and to model the imperfectly known temperature dependence of the semiconductor bandgap.

* Corresponding author. Address: Applied Physics Department, Universidad Politecnica Valencia, Pl. Ferrandiz i Carbonell, 2, 03801 Alcoy, Spain. Tel.: +34-96-652-84-42; fax: +34-96-652-84-09.
E-mail address: fjmanjon@fis.upv.es (F.J. Manjón).

0038-1098/$ - see front matter © 2003 Elsevier Ltd. All rights reserved.
doi:10.1016/S0038-1098(03)00616-1

2. Experimental procedure

The wurtzite ZnO single crystals used in this study were grown by chemical vapor transport after sublimation and oxidation of zinc (99.9995%) in a silica ampoule using ammonium chloride as a transport agent [7]. Four ZnO crystals with pure isotopic compositions ($^{64}Zn^{16}O$, $^{68}Zn^{16}O$, $^{64}Zn^{18}O$, and $^{68}Zn^{18}O$) and three with natural isotopic composition of Zn ($^{nat}Zn^{16}O$, $^{nat}Zn^{18}O$, and $^{nat}Zn^{16}O^{18}_{0.5}O_{0.5}$) were investigated. Low-temperature unpolarized PL experiments were performed with the seven samples in a backscattering geometry by placing them inside a helium close-cycle cryostat and using the 325.2 nm line of a He–Cd laser for excitation at power levels of 30 mW. The emitted light was analysed by a Jobin–Yvon HR460 spectrometer using a GaAs photomultiplier tube detector optimized for the UV–VIS range.

3. Results and discussion

The PL spectra at 15 K are dominated in all samples measured by a band around 369 nm (3.36 eV), which can be attributed to the emission of the I_4 bound exciton in which a neutral donor is involved [8,9]. Fig. 1(a) shows selected PL spectra of the $^{64}Zn^{16}O$, $^{68}Zn^{16}O$, $^{64}Zn^{18}O$ and $^{68}Zn^{18}O$ samples at 15 K, and Fig. 1(b) shows selected PL spectra of $^{nat}Zn^{16}O$, $^{nat}Zn^{16}O^{18}_{0.5}O_{0.5}$, and $^{nat}Zn^{18}O$ samples at 15 K. Due to the scatter of the measured values of the energies and linewidths of the bound exciton band for each isotopic composition, for the present study, we have taken as the nominal energy of the bound exciton for a definite isotopic composition the mean value of the energies measured for several samples with the same isotopic composition. In order to reduce the experimental scatter, we have used in our analysis the results obtained from samples with the narrowest peaks (FWHM < 5 meV) in the PL spectra. In this way, we have found that most of the average values agree with those observed for some samples except for the $^{nat}Zn^{16}O$ specimens. We have plotted in Fig. 1, the PL bands of samples whose bound exciton energies are close to the average value for each isotopic composition. A clear blue shift of the peak energy of the bound exciton luminescence is observed in all spectra when isotopic masses are increased.

Fig. 2 shows the dependence of the average peak energy of the bound exciton versus the total mass of the ZnO molecule. From the observed average energies, we have obtained several isotopic coefficients for the energy shift of the bound exciton with increasing isotopic mass ($dE_x/dM_{a,c}$, where the subindices a and c refer to the shift with the change of the anion or the cation mass, respectively). The different isotopic coefficients of the bound exciton energy are obtained from the slopes in Fig. 2 (straight lines) and given in parenthesis in that figure. Using isotopically pure

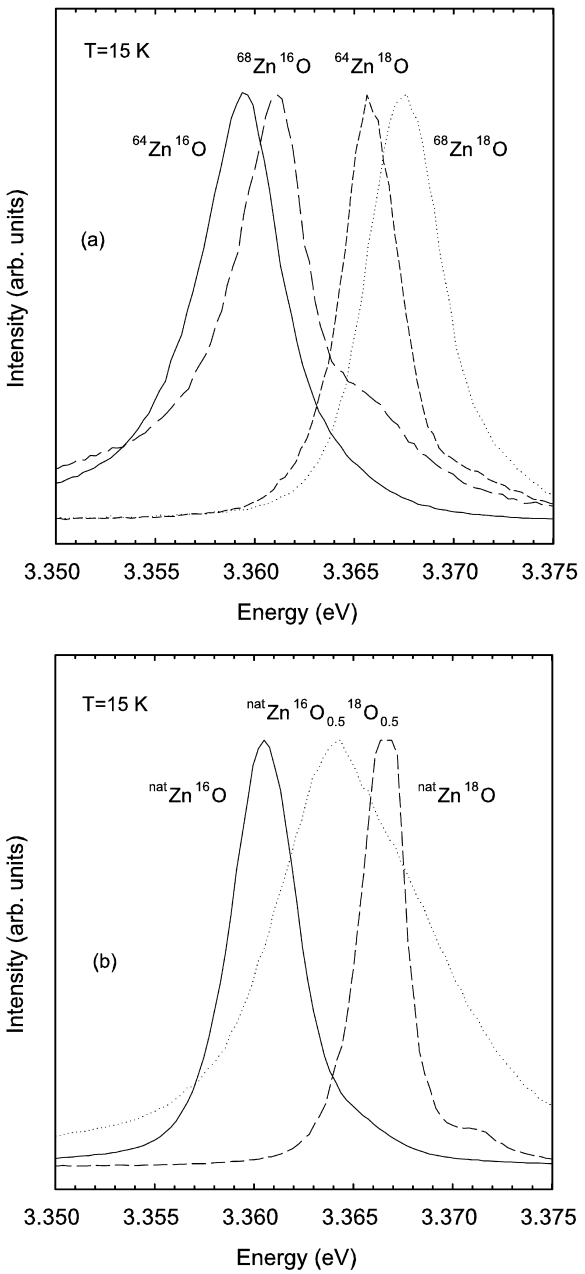

Fig. 1. (a) Selected photoluminescence spectra of isotopically pure ZnO samples at 15 K. (b) Selected photoluminescence spectra of ZnO samples with natural Zn composition and different oxygen isotopes at 15 K.

samples, we obtained a zinc isotopic coefficient $dE_x/dM_{Zn} = 0.40 \pm 0.03$ meV/amu when the Zn mass was changed and the oxygen mass remained equal to 16. The same Zn isotopic coefficient for a constant oxygen mass equal to 18 amounts to 0.43 ± 0.02 meV/amu. Additional natural isotopic samples lead to an average value of 0.41 ± 0.05 meV/amu. This value is close to that found

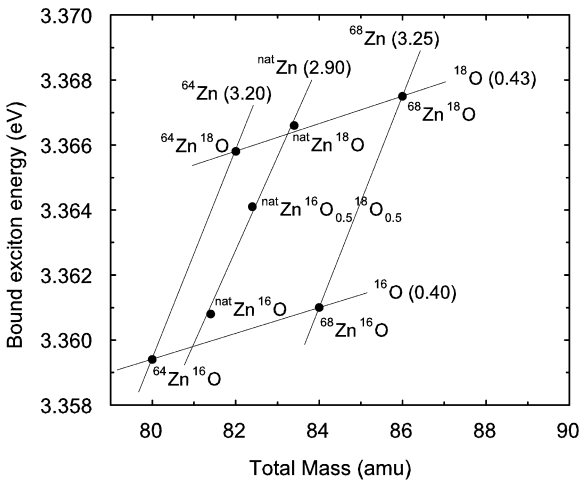

Fig. 2. Bound exciton energies of the seven measured isotopic samples of ZnO at 15 K. The nearly horizontal lines give the zinc mass coefficients of the bound exciton energy while the steep lines determine the oxygen mass coefficients of the bound exciton energy. The numbers in parenthesis are the zinc and oxygen mass coefficients (in meV/amu).

previously (0.375 meV/amu) for the change of the free A exciton with the Zn mass [5,6].

Using isotopically pure samples, we have obtained an oxygen isotopic coefficient $dE_x/dM_O = 3.20 \pm 0.08$ meV/amu by changing the O mass and keeping the zinc mass equal to 64. If the zinc mass is kept equal to 68, the oxygen coefficient amounts to 3.25 ± 0.06 meV/amu. The oxygen isotopic coefficient obtained from natural Zn samples is 2.90 ± 0.09 meV/amu, thus leading to an average value of 3.12 ± 0.11 meV/amu. Given the larger errors of the positions in natural samples, especially for $^{nat}Zn^{16}O^{18}_{0.5}O_{0.5}$, which has a larger linewidth than the other two, we believe that the best available value for the oxygen isotopic coefficient is 3.22 ± 0.10 meV/amu, which is similar to that found previously (3.4 meV/amu) for the change of the A exciton with the O mass [5,6].

The observed renormalization of the bandgap ΔE_g due to isotopic substitution is proportional to $M^{-1/2}$ and the difference between the zero-point bandgap renormalization energies for two different isotopic compositions can be described satisfactorily by the relation [2]

$$\Delta E_g(A) - \Delta E_g(B) = \Delta E_g\left(\frac{M(A) - M(B)}{M(A) + M(B)}\right), \quad (1)$$

where $\Delta E_g(A)$ and $\Delta E_g(B)$ represent the zero-point gap renormalization for two isotopes A and B with masses $M(A)$ and $M(B)$, respectively.

The energy difference of the average bound excitons for two different isotopes can be assumed to be equal to the l.h.s of Eq. (1) [3] and the knowledge of the isotopic masses of the two samples allows us to obtain the zero-point gap renormalization ΔE_g. Therefore, using the zinc isotopic coefficient (0.41 ± 0.05 meV/amu) and the oxygen isotopic coefficient (3.22 ± 0.10 meV/amu) we obtain a contribution of Zn to the renormalization energy $\Delta E_g(Zn) = -54 \pm 6$ meV and a contribution of O to that energy $\Delta E_g(O) = -110 \pm 3$ meV. Adding these contributions, a total gap renormalization energy at zero temperature $\Delta E_g = -164 \pm 9$ meV is found. This value is close to that estimated recently for GaN (-180 meV) [10] and midway between that of diamond (-334 meV) and that of either Ge or Si (-60 meV). We note, however, that the gaps of diamond, Ge and Si are indirect while that of ZnO is direct. Nevertheless, their phonon renormalizations are comparable in the manner described above.

In order to compare the gap renormalization value obtained for ZnO with those obtained from fits to the temperature dependence of the bandgap energy, we have measured the temperature dependence of the free A exciton in two samples ($^{nat}Zn^{16}O$ and $^{nat}Zn^{18}O$) between 15 and 300 K. Fig. 3 shows the PL spectra of the $^{nat}Zn^{16}O$ sample at different temperatures. The temperature dependence of the free A exciton in the $^{nat}Zn^{16}O$ sample is plotted in Fig. 4 together with data obtained by Harada et al. from ZnO particles embedded in an alkali halide matrix [11]. The temperature dependence of the free A exciton of $^{nat}Zn^{18}O$ (not shown in Fig. 3) is basically similar to that observed in

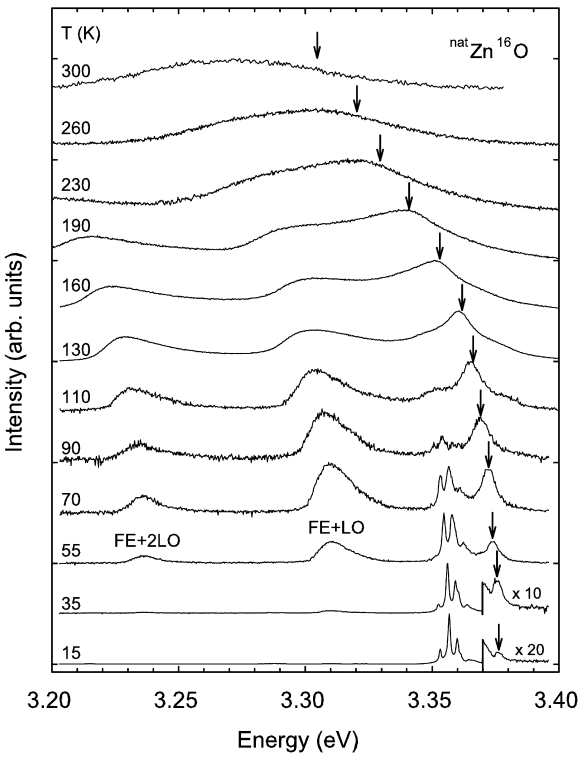

Fig. 3. Normalized photoluminescence spectra of natural ZnO at different temperatures between 15 and 300 K. The free A exciton emission (vertical arrows) and its phonon replicas are indicated. The peaks between 3.35 and 3.365 eV are located in the bound exciton region.

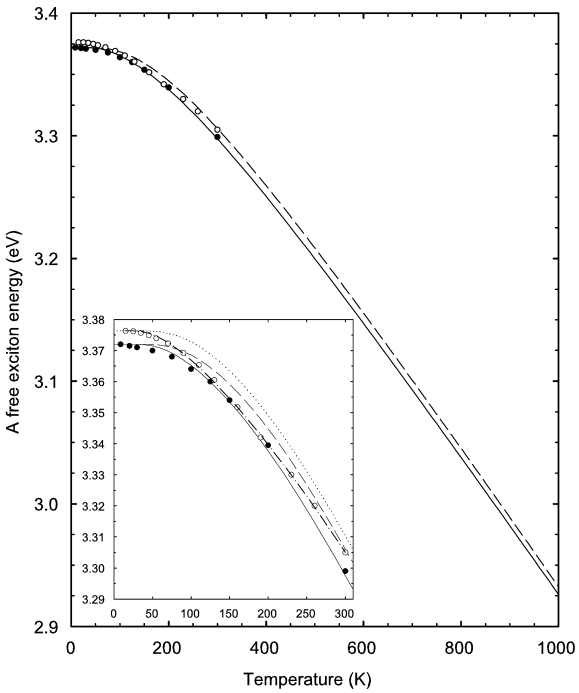

Fig. 4. Energy of the free A exciton in natural ZnO samples as a function of temperature up to 300 K. Blank circles correspond to our data while filled circles correspond to Harada's data [11]. The inset shows a zoom of the region of low temperatures up to 300 K. The solid and dashed-dotted lines correspond to fits of the data to a two-oscillator model according to Eq. (4), while dashed and dotted lines correspond to the two-oscillator model of Eq. (2) using the isotopic coefficients. The solid and dashed lines correspond to comparison with Harada's data whereas the dotted and dashed-dotted lines correspond to our data.

$^{nat}Zn^{16}O$, but shifted to higher energy. Just for comparison, the free A exciton energy in the $^{nat}Zn^{16}O$ sample at 15 K was measured to be at 3.3763 eV while that of the $^{nat}Zn^{18}O$ sample was measured at 3.3819 eV.

In order to compare the temperature dependence of the free A exciton with the behavior expected from the estimated partial (Zn and O) contributions to the gap renormalization energy, we use a two harmonic oscillator model [2,12,13]. In this model, the temperature dependence of the bandgap affected by the electron–phonon interaction is described by the interaction of electrons with two Einstein oscillators (representing basically an average acoustic and another average optic mode), whose effect depends on the phonon population through Bose–Einstein statistical factors. In the simplest approximation, we can use a longitudinal acoustic mode (LA) and a longitudinal optic mode (LO) [12]. The frequencies of the LA and LO modes depend mainly on the Zn and O masses, respectively, as suggested by recent ab initio calculations [14,15]. The acoustic phonon is mainly responsible for the bandgap shrinkage at low temperatures while the optic phonon gives a considerable contribution to the bandgap shrinkage at elevated temperatures. Within this model, the temperature dependence of the bandgap can be written as

$$E(T) = E_0 - 2M_{Zn}\frac{dE}{dM_{Zn}}\left[\frac{2}{\exp(\theta_1/T)-1}+1\right] - 2M_O\frac{dE}{dM_O}\left[\frac{2}{\exp(\theta_2/T)-1}+1\right], \quad (2)$$

where E_0 is the bare bandgap energy, dE/dM_{Zn} and dE/dM_O are the zinc and oxygen isotopic coefficients of the bandgap, and θ_1 and θ_2 are the average temperatures corresponding to the acoustic and optic phonon frequencies, respectively.

According to Eq. (2), the bandgap energy at $T = 0$ is

$$E(0) = E_0 - 2M_{Zn}\frac{dE}{dM_{Zn}} - 2M_O\frac{dE}{dM_O}. \quad (3)$$

For the calculations, we have taken the experimental isotopic coefficients obtained from the energy shifts of the bound exciton and assumed that the two phonons involved correspond to average frequencies of the acoustic and optic parts of the one-phonon DOS [16]. For the choice of these average frequencies, we confine ourselves to the LA and LO branches which have been shown to yield the main contribution to the gap renormalization in other similar semiconductors [12].

The average frequencies then become 240 cm^{-1} for the LA modes ($\theta_1 = 348$ K) and 550 cm^{-1} for the LO modes ($\theta_2 = 797$ K) [16]. The result of the calculations based on Eq. (2) using $E_0 = 3.372$ eV for Harada's data and 3.3763 eV for our data are plotted in Fig. 4 as dashed and dotted lines, respectively. Harada's data appear to fit slightly better the dependence suggested by Eq. (2), but unfortunately, our two-oscillator model based on the measured isotopic coefficients does not fit the low-temperature data. The reason is that Einstein oscillators leave out the long wavelength acoustic phonon density of states (Debye contribution). The calculated $E(T)$ so obtained is flatter than the experimental one [2]. This shortcoming can be palliated by using an additional low frequency oscillator representing the TA phonons [12]. We shall not do this here, however, in order to keep the number of free parameters under control. To improve on these fits it is clear that data on $E(T)$ for $T > 300$ K are needed. PL is not able to yield such data since the emission peaks are badly broadened already at 300 K. Conventional optical response techniques such as electroreflectance, should yield data for temperatures considerably higher than 300 K [17].

A fit of Harada's data with Eq. (2), but keeping the LO phonon frequency fixed ($\theta_2 = 797$ K) and leaving the acoustic phonon frequency as a free parameter gives a good agreement for $\theta_1 = 250$ K. This temperature corresponds to an average phonon around 160 cm^{-1} which is located near the centroid of the acoustic phonon DOS in ZnO [16]. This result suggests that both TA and LA phonons contribute appreciably to the temperature dependence of the bandgap in ZnO. We tried to follow the same procedure to

Table 1
Fit parameters of a two-oscillator model (Eq. (4)) to the temperature dependence of the graphs of natural ZnO samples from 10 K to room temperature obtained with fixed values for E_0 and θ_2. Harada's data for $^{nat}Zn^{16}O$ are from Ref. [11]. The average temperature Θ_{av} corresponds to the sum of the weighted θ_1 and θ_2 values. The values of the bandgap renormalization $E_{?0} - E(0)$ are also summarised

$^{nat}Zn^{16}O$	$T_{min} - T_{max}$ (K)	$E(0)$ (eV)	$\alpha/10^{-4}$ (eV/K)	w_1	θ_1 (K)	θ_2 (K)	Θ_{av} (K)	$E_0 - E(0)$ (meV)
Harada	8–300	3.3720	6.98	0.26	149.8	797	628.7	−219
Ours	15–300	3.3763	4.50	0.64	194.3	797	411.3	−92

fit the temperature dependence of the energy gap of our natural sample, however we did not succeed in obtaining a reasonable result.

For the sake of comparison, we have also tried to fit our and Harada's data with a two-oscillator model using four adjustable parameters, as suggested by Pässler [13].

$$E(T) = E_0 - \alpha\left[w_1\theta_1\left(\frac{1}{\exp(\theta_1/T)-1}+\frac{1}{2}\right) + (1-w_1)\theta_2\left(\frac{1}{\exp(\theta_2/T)-1}+\frac{1}{2}\right)\right], \quad (4)$$

where E_0, θ_1 and θ_2 have the same meanings as in Eq. (2), α is a coupling factor and w_1 is a weighting factor ($0 < w_1 < 1$) which determines the strength of the coupling to each of the two oscillators. Fitting Harada's and our data to Eq. (4) leaving as free parameters α, w_1 and θ_1 and fixing E_0 and $\theta_2 = 797$ K, we obtain respectively, the solid and dashed-dotted lines plotted in Fig. 4. The fit parameters are listed in Table 1. Pässler's two-oscillator fit to our data yields a zero-temperature renormalization energy of $\Delta E_g = -92$ meV for $^{nat}Zn^{16}O$, while the same fit to Harada's data yields a zero-temperature renormalization energy $\Delta E_g = -219$ meV. The renormalization energy we estimate for ZnO from isotopic shifts (−163.6 meV) lies half way between these two estimates, a fact which emphasizes the instability of such fits within the low temperature range for which PL data are available.

4. Conclusions

In this work, we have reported a detailed study of the low-temperature PL of seven unintentionally doped ZnO samples with different isotopic compositions. As a result, we have obtained the zinc and oxygen isotopic coefficients from the isotopic shift of the bound exciton energy in agreement with those previously obtained for the shift of the free A exciton energy. The temperature dependence of the free A exciton energy of some samples has also been measured by PL and compared with other recent data. Available data (for $T < 300$ K) for the temperature dependence of the free A exciton energy, and consequently of the bandgap, can be represented by a two-oscillator model incorporating the isotopic coefficients. The results of the two-oscillator model proposed here are compared with the results obtained by fitting the temperature data with a four-parameter two-oscillator model previously proposed. Both models seem to describe fairly well the temperature dependence experimentally observed.

Acknowledgements

The authors thank Dr Christian Bernhard for a critical reading of the manuscript and R. Pässler and A. Segura for informative discussions. This work was supported through Spanish Government MCYT grant MAT2002-04539-C02-02 and Generalitat Valenciana OCYT grant GV01-211. F. J. M. acknowledges financial support by the "*Programa Incentivo a la Investigación de la U.P.V.*".

References

[1] S.R. Ahuja, L. Farst, O. Ericson, J.M. Willis, B. Johannson, J. Appl. Phys. 83 (1998) 8065 for a collection of references related to applications.
[2] M. Cardona, Phys. Status Solidi b 220 (2000) 5.
[3] T.A. Meyer, D. Karaiskaj, M.L.W. Thewalt, M. Cardona, Solid State Commun. 126 (2003) 119.
[4] D. Olguin, M. Cardona, A. Cantarero, Solid State Commun. 122 (2002) 575.
[5] F.I. Kreingol'd, Fiz. Tverd. Tela 27 (1978) 3138 Sov. Phys. Solid State 20 (1978) 1810.
[6] F.I. Kreingol'd, B.S. Kulinkin, Fiz. Tverd. Tela 28 (1986) 3164 Sov. Phys. Solid State 27 (1986) 1781.
[7] R. Lauck, private communication.
[8] V.A. Nikitenko, A.I. Tereshchenko, Opt. Spectrosc. 47 (1979) 671.
[9] R. Heitz, C. Fricke, A. Hoffmann, I. Broser, Mater. Sci. Forum 83–87 (1992) 1241.
[10] R. Pässler, Phys. Rev. B 66 (2002) 085201.
[11] Y. Harada, H. Kondo, N. Ichimura, S. Hashimoto, Jpn. J. Appl. Phys. 38 (1999) L1318.
[12] J. Serrano, C. Schweitzer, C.T. Lin, K. Reimann, M. Cardona, D. Frohlich, Phys. Rev. B 65 (2002) 125110.
[13] R. Pässler, J. Appl. Phys. 89 (2001) 6235.
[14] J. Serrano, F. Widulle, A.H. Romero, A. Rubio, R. Lauck, M. Cardona, Phys. Status Solidi b 235 (2003) 260.
[15] J. Serrano, PhD Thesis, University of Stuttgart, 2003 (unpublished).
[16] J. Serrano, F.J. Manjón, A.H. Romero, F. Widulle, R. Lauck, M. Cardona, Phys. Rev. Lett. 90 (2003) 055510.
[17] M. Cardona, K.L. Shaklee, F.H. Pollak, Phys. Rev. 154 (1967) 696.